LONDON, METEOROLOGICAL OFFICE.

Met.O.15 Internal Report No.48.

Three case studies of shallow convection using a tethered balloon. By KITCHEN,M., LEIGHTON,J.R. and CAUGHEY,S.J.

London,Met.Off.,Met.O.15 Intern.Rep.No.48, 1982,32cm.Pp.[32].14 pls.27 Refs.Abs.p.1.

METEOROLOGICAL OFFICE
London Road, Bracknell, Berks.

MET.O.15 INTERNAL REPORT

No 48

THREE CASE STUDIES OF SHALLOW CONVECTION USING A TETHERED BALLOON

BY

M KITCHEN, J R LEIGHTON AND S J CAUGHEY

January 1983 Cloud Physics Branch (Met.O.15)

SUMMARY

Aspects of the dynamical and microphysical structure of three cloudy boundary layers have been investigated using tethered balloon-borne instrumentation. The types of cloud studied ranged from small thin cumulus to medium cumulus (non precipitating) and stratcumulus formed by the spreading out (shelving) of cumulus. Available synoptic data has been used to show the importance of advection and subsidence over horizontal scales of order 100 km on the local boundary layer development. The factors which influenced the extend of cloud cover are discussed along with the effect of condensation on vertical air motions in the upper half of the convective boundary layer. Horizontal variations in cloud droplet spectra were similar in each of the cases, with no systematic differences in the effects of the mixing of dry air into cloud attributable to differences in other measured parameters. Horizontal variability of the spectra within individual clouds were related to position within the cloud and height above the local cloud base.

1. INTRODUCTION

Many previous studies of cumulus clouds formed in the convective boundary layer (CBL) have been either confined to the structure of the individual clouds (eg. the comprehensive observations of Warner 1969, 1969a, 1970, 1973, MacPherson and Isaac 1977) or else the thermodynamic structure of the cloud environment (eg. Coulman and Warner 1977). Recently however more complete case studies of cumulus in the CBL have been made (Lemone and Pennel 1976) in which both cloud and sub-cloud layers are described. Similarly there have been a number of case studies of marine stratocumulus (Slingo et al 1982b and Brost et al 1982) which have used aircraft to make comprehensive measurements. To date, however there have been few comparable data obtained over land. Tethered balloon instrumentation has some advantages over aircraft instrumentation for making such studies (Kitchen and Caughey 1981, hereafter referred to as I) and recent work using such instrumentation has included measurements in nocturnal stratocumulus (Roach et al 1982), small cumulus (I) and medium sized maritime cumulus clouds (Emmitt, 1978). The work presented here represents an extension of the experiment described in I to a wider range of cloud types in order to establish whether the conclusions from I are generally applicable.

One of the conclusions of the noctural stratocumulus studies (Roach et al 1982) was that variations in the subsidence velocity on a horizontal scale of about 100 km played an important role in controlling the depth of the cloud layer. In the daytime CBL in summer, entrainment of air from above the inversion is likely to be the major influence in determination of the cloud layer depth, not only through changes in the inversion base height but also through the entrained heat and moisture fluxes. In section 3 of the present paper, an attempt to determine the relative effects of entrainment and subsidence is described.

Entrainment and subsidence may also change the fractional cloud cover in the CBL. In turn, changes in cloud cover may affect the CBL structure through

changes in latent heat released in the cloud layer and the amount of surface heating. Such interactions are too complex to resolve using presently available data, but as one of the case studies included a transition from isolated cumulus to stratocumulus cloud cover, the opportunity has been taken to identify changes in the CBL which may influence the degree of shelving (see section 4).

The location of clouds within the CBL has been shown to be intimately connected with convective air motion in the sub-cloud layer (see eg. Lemone and Pennel 1976 and Emmitt 1978). In I, marked coherence between vertical velocity measurements at levels separated by several hundred metres in the vertical was found. Similar coherence was found in the present study and the correlation between air motions at different levels quantified. Also in I, the profile of vertical velocity variance, computed over a sufficient length of time to include scales of a few km, was shown to be similar to those obtained from the clear air CBL. Within cloud, there was considerable enhancement of small scale (< 50 m) turbulence, but this was insufficient to cause significant enhancement vertical velocity variance computed over < 10 km within the cloud layer. A question which arises from this conclusion is what (if any) scale of clouds cause a significant enhancement of mean vertical velocity variance in the cloud layer? This question is answered (see section 5) for the range of cloud types sampled in these present studies.

Within individual cumulus clouds, the air motion on the convective scale (of order 500 m) has been shown to be highly organised, with similar flow patterns being observed in a number of different clouds (see I). Similar organisation on this scale has been observed in nocturnal stratocumulus layers (Caughey et al 1982 and Caughey and Kitchen 1983). The convection in the latter case arising from the radiative loss from near to cloud top leading to a sensible heat flux within the cloud layer. Brost et al (1982) have pointed out that the radiative loss from near the top of layer cloud, need not necessarily result in convection in the cloud layer if the loss is balanced by either entrainment or else a flux of liquid water away from cloud top. Slingo et al (1983) suggested that in

daytime stratocumulus, a combination of longwave loss from cloud top and shortwave absorption nearer to cloud base would lead to enhanced convection within cloud. The convective air motions within individual cloud elements in the present studies are described in section 6.

As a result of the organised motion in nocturnal stratocumulus Caughey and Kitchen (1983) found horizontal variations in droplet specra. Similarly, variability in spectra related to the air motions within marine stratocumulus has been found by eg. Brost et al (1982). To date, no similar variability linked to dynamical structure has been found within cumulus clouds, and both Warner (1981) and Telford and Wagner (1980) stressed the need for droplet data with a high spatial resolution in order to resolve the liquid water distribution within cloud satisfactorily. The present observations provide such data, albeit for a limited number of clouds. Some of the problems which may arise in the interpretation of droplet data of lower resolution than in the present case are highlighted.

One of the causes of horizontal variability in droplet spectra in the horizontal is the effect of mixing between cloudy and clear air. The model of mixing first developed by Latham and Reed (1977) has been shown to account for the variability in spectral shape in a variety of cloud types (see eg. I, Caughey and Kitchen 1983, Slingo et al 1982b). More recently, the model has been further developed (baker et al 1980, Baker and Latham 1982) and the extent to which the mixing will approximate to the "extreme inhomogenous" description whown to depend on the nature of the entrainment. This more sophisticated treatment has been used to account for observed differences between the effect of mixing in different cases (Blyth et al 1980). The present data have been used to determine whether predictions of this model can be further validated by finding systematic differences in droplet spectra variability between different case studies.

2. INSTRUMENTATION AND EXPERIMENTAL DETAILS

The balloon-borne instrumentation was the same as that used in a previous experiment and has been fully described in I. Only a brief description is given here and for further details, the references given in I should be consulted.

Three turbulence probes and a PMS* ASSP-100 droplet spectrometer were mounted on the tethering cable of a 1300 m^3 balloon. The probes were spaced about 250 m apart and the ASSP positioned 3 m above the uppermost probe. The turbulence dataset considted of the three orthogonal wind components (u, v, w) and the temperature (T). The analogue output was subsequently sampled at a rate of 20Hz, digitised, and then filtered at a 10Hz rate to provide some initial smoothing. Each droplet spectrum recorded from the ASSP was accumulated over a period of one second. Time synchronization between the ASSP and turbulence probes was established to within ± 1s over the observation periods.

This basic instrumentation was supplemented by visual observations of those clouds which passed above or through the instrument array. Written notes and photographs enabled a description of many of these clouds to be made. Flags positioned at approximately 150 m intervals on the tethering cable were used to estimate the cloud base height to within ± 50 m. Other instruments at the same site used in the experiment were a solarimeter measuring total incoming solar radiation and a lysimeter providing evaporative heat flux measurements (see Roach et al 1982).

The experiments were conducted at RAF Cardington, Beds and the three particular case studies descirbed refer to observations made on the 18, 19 and 21 August 1980 (referred to as those of the 18, 19 and 21 hereafter). During the observation period on each of these days, the instruments were raised steadily up through the CBL and then a series of level runs were made with the uppermost turbulence probe usually within the cloud layer but sometimes above it. At the end of the period, the instruments were profiled back down to the surface

---

* Particle Measuring Systems Inc, Boulder, Colorado

(see Fig. 1).

During the late afternoon of the 19, the turbulence probes were mounted side by side at a height of 2 m above the surface and an intercomparison lasting about 90 minutes was made to assess the errors arising from differences between the probes. Table 1 shows the averages from this run of those parameters used later in the analysis. In consideration of the data from runs made at altitude however, two additional sources of error arise.

a) The temperature sensor on each probe was a platinum resistance wire which was subject to wetting within cloud. Hence temperatures measured within cloud will have tended towards the wet bulb with possible spurious effects near cloud boundaries due to evaporation.

b) The ASSP was mounted on a boom which was attached to both the balloon tethering cable, and also by cables to other points on the balloon centreline. This method of mounting was designed to align the ASSP with the wind direction. Acrosswind motion of the balloon caused the boom to swing and in an attempt to reduce these oscillations a small drogue parachute was attached to the boom on the 18. Unfortunately, the drogue caused vibrations in the tethering cable which contaminated the turbulence probe wind components with an oscillation of about 1 second period. The amplitude of the variations in w arising from this cause were such that only the high frequency (> 0.5 Hz) part of the vertical velocity power spectrum was affected, but the total variance, computed over times of order 20 minutes, was much larger than the variance due to these spurious oscillations. No detrimental effect upon the ASSP measurements were detected as a result of omission of the drogue.

The droplet sizing capabilities of the ASSP have been proven by many comparisons with other instruments (see I). However, it is recognised that the droplet concentration (and hence liquid water content derived from integration of the spectra) may be subject to systematic error, principally due to uncertainties in the sampling volume. In order to improve the

concentration estimates presented here, a correction factor was calculated as follows. Data from two days on which measurements were made within layer cloud were studied and times selected when the ASSP was well above cloud base and within an updraught. The liquid water content in these regions, calculated from integration of the droplet spectra, was corrected to the adiabatic value using estimates of cloud base height. The average correction factor for droplet concentrations was estimated to be a multiplication by 3.5, very similar to corrections for the ASSP derived by Slingo et al (1982). This factor is subject to uncertainty from errors in the cloud base estimates and in the assumption that peak liquid water contents were adiabatic. It is not intended to provide accurate concentrations, but to provide more realistic estimates for presentation. Quantitative interpretation of the droplet data has been confined to relative quantities which do not rely on the accuracy of this correction.

3. SYNOPTIC SCALE INFLUENCES ON THE CLOUD LAYER

(a) Synoptic background to the case studies

During the period covering the three case study days (18-21 August 1980), south-east England lay on the NE flank of an anticyclone centred south-west of Ireland. North-westerly flow was therefore maintained across southern districts throughout this period. On the 18, a satellite picture taken at 1430 GMT (Fig.2) shows extensive cumulus development over the land area with the convective activity declining towards the south-east. In the vicinity of Cardington, upwind the cumulus clouds appear to be grouped into patches of a scale about 10 km across, whilst downwind, the clouds are banded into streets orientated approximately alongwind with a spacing of approximately 5 km.

On the 19, a weak ridge developed ahead of a warm front approaching from the north-west which brought air over the Cardington area from a more westerly direction with higher surface dew points than on the previous day. Areas of thin medium level cloud obscured most of the low level cloud over southern England on the satellite picture so a conventional nephanalysis of low cloud amounts based

surface observations is shown in Fig. 3. Most of southern England at 1200 GMT was covered by $> {}^{4}/_{8}$ cumulus or stratocumulus with Cardington itself lying in a large area covered by $\geq {}^{6}/_{8}$ stratocumulus. Cloud amounts at Cardington increased throughout the day before declining during the late evening.

The passage of the warm front was followed by the associated cold front which passed through Cardington during the early morning of the 21., The front was weak in that only light rain fell in the area, but it did mark a strong temperature change. Screen temperatures during the daytime on the 21 were lower than the minimum on the previous night. The anticyclone reasserted its influence during the 21 and the satellite picture (Fig. 4) taken at 1358 GMT shows only small amounts of cumulus over southern England with cloud streets upwind of the Cardington area with a spacing of about 5 km (measured from the satellite photograph).

Data from the 1100 GMT Crawley radiosonde ascents (about 100 km south of Cardington) for the 18, 19 and 21 are shown in Fig. 5. The temperature and humidity profiles are typical of the well mixed CBL and the increasing strength of the capping inversion during this period can also be seen. Little windshear was evident on the 18 or 19 but on the 21, when windspeeds were about 3 ms^{-1} higher than in the other two cases, there is evidence of an increase in windspeed with height near the CBL top with a similar decrease just above the inversion layer top.

In summary, the synoptic conditions on the three days of the case studies were typical of anticyclonic type weather over the British Isles in summer , with shallow convective cloud formed at the top of a well mixed CBL capped by a subsidence inversion.

(b.) Boundary layer development

Changes in the boundary layer depth arise from three sources, namely entrainment, subsidence and advection. Defining vertical motion upwards as being positive, then the local change in CBL depth is given by:

$$dz_i/dt = w_e + w_s + \bar{U}dz_i/ds \quad \ldots\ldots \quad (1)$$

where dz_i/ds is the slope of the inversion in the upwind direction and the remaining symbols are defined in the list at the end of the paper. Roach et al (1982) in a study of nocturnal stratocumulus found that variations in w_s on a horizontal scale of order 100 km caused modulations in the depth of the cloud layer and the dispersal of cloud in some areas. The effects of advection and entrainment, although important in the heat and moisture budgets of the boundary layer, were of lower magnitude than subsidence over the timescale of their observations (a few hours). However in the daytime CBL, entrainment rates are typically larger, particularly during the morning when inversion rise is most rapid. Caughey and Palmer (1979) reported values of w_e of $-.08\ ms^{-1}$ in clear CBL's over central England in summer. (Cf. an estimate of w_e in a nocturnal stratocumulus case of about $-0.005\ ms^{-1}$ (Roach, 1982)). With entrainment velocities of this order, w_e would dominate the right hand side of eqn. 1. In two of the present cases estimates of dz_i/dt, $\bar{U}dz_i/ds$ and w_s have been made to assess the relative magnitudes of entrainment, subsidence and advection to establish whether subsidence was an important effect on the cloud layer depth in the daytime CBL.

During the early part of the observation period on the 19, cloud base height z_b was observed to rise steadily from 750 m at 0900 GMT to about 1300 m by 1030 GMT. During this period, the depth of the cloud layer was (estimated from photographs) not seen to increase significantly and so we may deduce that z_i was increasing at approximately the same rate as z_b. The error in dz_i/dt for this period shown in Table 3 is based upon a 100% change in cloud layer depth occurring during this time. Thereafter, frequent traverses of the inversion layer were made by the uppermost probe and z_i was only observed to increase by about 60 m during the period 1030-1240 GMT (see Table 2). In order to estimate w_s, fields of surface divergence were calculated from surface wind observations using the objective scheme devised by Purser and McQuigg (1982) and previously used for a similar purpose with some success by Roach et al (1982). The divergence pattern over eastern England at 1200 GMT on this day was rather

weak with values lying between 0 and $10^{-5}s^{-1}$(Fig. 6a). If the latter value was maintained throughout the depth of the CBL, the implied w_s would be -.01 ms^{-1} but the likely error on this figure is difficult to estimate. The advection term in Eqn. 1 was estimated by taking the 1100 GMT radiosonde ascents at Aughton and Crawley (positions shown in Fig. 3) as being representative of upwind and downwind conditions respectively and comparing the inversion base heights with that at Cardington. Thus two values of $\bar{U}dz_i/ds$ were calculated providing some estimate of the error. The magnitude of individual terms in eqn. 1 are shown in Table 3, along with a value of w_e calculated as a residual. It seems probable that the rise of the inversion between 0900 and 1030 GMT on the 19 was therefore due to entrainment and the subsequent halt in boundary layer growth implies a sudden decrease in the entrainment velocity. It is of interest that around the same time (1030 GMT) there was an increase in cloud cover at Cardington from about $^3/_8$ cumulus to $^7/_8$ stratocumulus. (See Fig. 1) Possible reasons for this transition are discussed below.

On the 21, the CBL was observed to increase steadily in depth throughout the observation period with an estimated mean value of dz_i/dt = .02 ms^{-1} (Table 3). Cloud amounts remained small with a maximum of $^3/_8$ scattered cumulus at 1100 GMT but generally < $^1/_8$ (Fig. 1). The terms in eqn. 1 were calculated in the same way as for the 19 and are given in Table 3. In this case, the advection term made a significant positive contribution to dz_i/dt and combined with entrainment resulted in a steady growth in the CBL, despite the greater subsidence than on the 19. Comparison between the satellite picture (Fig. 4) and the surface divergence pattern (Fig. 6b) show some degree of correlation between subsidence and cloud amounts on scales of order 100 km. For example, the broad cloud free area across southern England corresponds to an area of positive divergence at the surface whilst a smaller area of enhanced convective activity over the east coast in the upper half of Fig. 4 corresponds to a similar sized area of negative divergence. Small spatial variations in z_i caused by variations in w_s can have a relatively larger effect on the depth of the cloud layer if the

liquid water content of the clouds is a small fraction of the adiabatic value than if it approaches the adiabatic value. If the cloud top is displaced downwards by a distance Δz_i, then the cloud base will rise by an amount Δz_b, given by (see Roach 1983)

$$\Delta z_b = (1 - {}^{1}/_{\alpha})\, \Delta z_i \qquad \ldots\ldots \qquad (2)$$

Cumulus clouds observed at Cardington on the 21 were about 100 m in depth. If we take a valueof $\alpha = 0.5$ as being typical (see eg.I) and $w_s = -.01\ ms^{-1}$ then the effect of subsidence alone would be to dissipate the clouds in slightly more than one hour. A strong correlation between cloudiness and divergence is therefore probable even in the daytime CBL if the cloud layer is shallow. Roach et al (1982) speculated that the origin of divergence variations in their particular case in southern England may have been topography. Although the cloud cover in north-west England was associated with high ground on the 21 (see Fig. 4) there is no evidence that the same is true in the south-east of England.

4. THE EXTENT OF CLOUD IN THE CBL

The cloud cover in the CBL during these studies ranged from $< {}^{1}/_{8}$ to ${}^{7}/_{8}$, with large changes in cover occurring over a period of about an hour on the 19 as a result of spreading of cumulus clouds into stratocumulus patches. Ludlam (1980) identifies the moisture distribution in the cloud layer as determining the degree of shelving of cumulus clouds, with three factors likely to promote spreading:-

(i) Minimal drying of the CBL due to large scale subsidence

(ii) A low Bowen ratio

(iii) A low entrainment rate into the CBL, probably associated with a low windshear across the capping inversion.

Once the cumulus beings to shelve, then there is a feedback mechanism will act to increase cloud cover further. A decrease in surface insolation reduces the surface sensible heat flux. The reduced convection will tend to result in a lower entrainment rate because of the reduced bombardment of the inversion by thermals. This will in turn tend to increase the moisture flux convergence in the

cloud layer. Ludlam (1980) suggested that because of the feedback mechanism and because the moisture flux convergence in the CBL depends on a delicate balance between evaporation and entrainment, then the exact cause of a change in cloud cover would be difficult to determine.

The case study on the 19 provides an opportunity to study the rapid shelving of cumulus cloud, and to see whether the factors identified by Ludlam were acting to favour of such an increase in cloud cover. Looking at each of these factors for the period 1030-1230 in turn:-

(i) From Table 3, w_s on the 19 was close to zero.

(ii) The measured surface fluxes during three hour periods on the case study days are shown in Table 4. In the time 0900-1200 on the 19, $S_o - E_o = 190$ Wm^{-2} whereas in the following three hours, this had fallen to 140 Wm^{-2}. This decline is likely to have resulted in a larger fractional decrease in the surface sensible heat flux than the decrease in evaporative latent heat flux and thus decreased the Bowen ratio. During the probe intercomparison (see section 2) at about 1500 GMT on this day, the surface sensible heat flux measured by the eddy correlation method was 5.8 $\pm$ 2.2 Wm^{-2} suggesting that by this time, the Bowen ratio was perhaps as low as .03.

(iii) As described in the previous section, there is evidence that a decrease in the magnitude of the entrainment velocity occurred at about the same time as cloud cover increased (Table 3).

Therefore all these factors were acting to increase cloud cover, but because their interdependence cannot be quantified using the available data, the causal factor is not known. We can however estimate the latent heat flux convergence using the values of w_e in Table 3, E_o in Table 4 and Δq from the Crawley radiosonde ascents (Fig. 5). Estimates of the entrained latent heat flux on the 19 and 21 are given in Table 4 and suggest that there was approximate balance between evaporation from the surface and entrainment except during the afternoon of the 19. It must be admitted however that the errors in these figures may be large, bearing in mind the possible errors in w_e (Table 3). There is also evidence, for a decline in the

entrained sensible heat flux on the 19, not only because of the reduction in entrainment, but also the magnitude of the temperature step across the inversion decreased, with time, (see Table 2). This would tend to increase the relative humidity in the CBL by reducing the rate of rise in mean CBL temperature.

In contrast to the clouds on the 19, those which formed on the 21 were very small and of short lifetime (about 10 minutes). Despite the steady increase in boundary layer depth, the depth of cloud did not increase significantly (see Fig. 1). Because of the extreme dryness of the air above the inversion (Fig. 5) the entrained latent heat flux probably closely balanced the surface evaporation (see Table 4) and also resulted in any parcels of air which were entrained into the CBL from above sinking unstably down through the cloud layer. On the 21 the θ_e profile (Fig. 5) had a minimum located above the inversion. Such entrainment instability may have acted to quickly mix entrained dry air throughout the cloud layer. In contrast, on the 18 and 19, θ_e increased through the inversion layer, thus air entrained into cloud from above the inversion would not sink unstably and the evaporation of cloud due to mixing of air from above the inversion would tend to proceed more slowly.

5. VERTICAL VELOCITY FLUCTUATIONS ON CONVECTIVE AND TURBULENCE SCALES

In this section we examine the larger scale (greater than about 200 m) up and downdraught structure and also the distribution of small scale (< 50 m) turbulence.

The level runs in these cases were generally less than one hour in duration (see Fig. 1) ie. they represent an alongwind sample of less than 20 km in length. Power spectra of vertical velocity obtained by a fast Fourier transform method showed considerable scatter at the low frequency end of the spectrum (equivalent to scales > a few hundred metres) because of the small number of convective up and downdraughts sampled in each run, and also because they were rather randomly distributed in time. For these reasons a much more simple form of scale analysis was performed in which for each of the 3 probe levels, 20 second mean vertical velocities (ie. mean over 100-200 m) were computed after subtracting the mean for

each level run. Then using a mean windspeed for each case study, the sizes of individual updraughts sampled ($w > 0$ ms^{-1}) were calculated and placed into one of three size classifications (< 1 km, $\geqslant$ 1 km but $\leqslant$ 2 km, > 2 km). The extra complication of using the mean windspeed for each level and each run would not be justified in view of the coarseness of the classification and the relatively small fractional changes in windspeed which occurred during each day. The proportion of the total level run time occupied by updraughts of each size range was totalled and the results shown in Fig. 7. (Insufficient vertical velocity data were obtained from the uppermost probe on the 21 to be presented). In the same way, the scale of individual clouds which passed either directly above or through the instrument array was calculated from visual observations and placed in the same categories. It can be seen that the distribution of updraught scales on the 18 and 19 bore little relationship to the cloud scale distribution. During about 40% of the level run time on the 19, the instruments were within or beneath patches of cloud > 2 km in extent whereas none of the updraughts intercepted was as large as this. The other feature of these data is the difference in the updraught scales between the two levels in the sub-cloud layer and the level in the cloud layer.

In the case study described in I, a subjective assessment of the vertical velocity traces suggested a marked coherence between vertical velocities at levels about 300 m apart in the upper half of the CBL. In the present case, there was a similar correlation apparent between the vertical velocity time histories from the different probes. Using the 20 second means of vertical velocity and taking all the level run data from each case study together, the correlation coefficients between the different levels were calculated. Although most of the main up and downdraughts were evident in the vertical velocity traces at all three levels, time lags resulted in rather low values of the coefficients. Between adjacent levels the correlations were all within the range 0.25 to 0.5, but fell to between 0.1 and 0.2 between top and bottom levels (about 500 m vertical separation).

Profiles of vertical velocity variance, σ_w^2, computed over a long averaging period in the clear air CBL show a strong decrease with height as the inversion

each level run. Then using a mean windspeed for each case study, the sizes of individual updraughts sampled ($w > 0$ ms^{-1}) were calculated and placed into one of three size classifications (< 1 km, $\geqslant 1$ km but $\leqslant 2$ km, > 2 km). The extra complication of using the mean windspeed for each level and each run would not be justified in view of the coarseness of the classification and the relatively small fractional changes in windspeed which occurred during each day. The proportion of the total level run time occupied by updraughts of each size range was totalled and the results shown in Fig. 7. (Insufficient vertical velocity data were obtained from the uppermost probe on the 21 to be presented). In the same way, the scale of individual clouds which passed either directly above or through the instrument array was calculated from visual observations and placed in the same categories. It can be seen that the distribution of updraught scales on the 18 and 19 bore little relationship to the cloud scale distribution. During about 40% of the level run time on the 19, the instruments were within or beneath patches of cloud > 2 km in extent whereas none of the updraughts intercepted was as large as this. The other feature of these data is the difference in the updraught scales between the two levels in the sub-cloud layer and the level in the cloud layer.

In the case study described in I, a subjective assessment of the vertical velocity traces suggested a marked coherence between vertical velocities at levels about 300 m apart in the upper half of the CBL. In the present case, there was a similar correlation apparent between the vertical velocity time histories from the different probes. Using the 20 second means of vertical velocity and taking all the level run data from each case study together, the correlation coefficients between the different levels were calculated. Although most of the main up and downdraughts were evident in the vertical velocity traces at all three levels, time lags resulted in rather low values of the coefficients. Between adjacent levels the correlations were all within the range 0.25 to 0.5, but fell to between 0.1 and 0.2 between top and bottom levels (about 500 m vertical separation).

Profiles of vertical velocity variance, σ_w^2, computed over a long averaging period in the clear air CBL show a strong decrease with height as the inversion

base is approached (see eg Caughey and Palmer 1979). The profile given in I showed a similar decrease which suggested that small cumulus did not cause an increase in variance in the cloud layer through the release of latent heat. In the present cases, σ_w^2 was computed from sections of the level runs shown in Fig 1. The sections were of unequal length (about 15 to 60 mins) and hence some scatter in the results may result from the different amounts of spectral loss at low frequencies. Each value of σ_w^2 was then corrected for the differences between the variances measured by the probes in the ground run (see section 2). It was assumed that these differences arose from linear variations in the response of the vertical velocity sensors and proportionality constants derived from the data in Table 1 have been used to correct the values of σ_w^2 measured by probes 1 and 3 (ie probe 2 was arbitrarily considered to be accurate). The resulting profiles of σ_w^2 (Fig 8a) are similar to those in I and Caughey and Palmer (1979), and no clear evidence emerges for an enhancement of horizontally averaged vertical air motion within the cloud layer, even in the case of medium sized cumulus on the 18. Of some interest, however, is the decrease in σ_w^2 in the upper half of the CBL during the observation period on the 19. This change was probably as a result of the reduction in surface insolation (due to increasing cloud cover) causing a similar decrease in the sensible heat flux (see section 4).

The dissipation rate of turbulence kinetic energy, ε, was computed from the spectral density of vertical velocity at a frequency of 1 Hz (see I). The profiles of ε (Fig 8b) are very similar to those of σ_w^2 (Fig 8a) and illustrate the effectiveness of the inversion layer in damping out vertical velocity fluctuations on scales of order 10 m, as well as on the scale of the convective up and downdraughts.

Several workers have found an enhancement in small scale turbulence within clouds in the CBL (see eg I, Silayeva and Shmeter 1977, MacPherson and Isaac 1977). The present case studies provide an opportunity to try and

and relate such enhancement to the size of the clouds. Values of σ_w^2 were computed over about (6 second) averaging periods and then those segments from within cloud (as detected by the ASSP), beneath cloud, or between clouds were grouped together and averaged. The results (Table 5) for the 19 and 21 demonstrate the highly variable nature of the turbulence on this scale with variations in σ_w^2 within each group being of the same order as the mean value, despite the mean representing averages over at least 25, 6 second periods. Any firm conclusions based on these results is therefore precluded but there is evidence of enhanced turbulence within the clouds (only the top level was usually within the cloud layer) on both the 19 and 21 and also beneath the cloud areas on the 19. An additional statistic is that out of 13 cumulus clouds analysed, in only 5 was the mean small-scale turbulence (averaged over the time the uppermost probe was within cloud) higher than the mean from the same time period at the level beneath cloud base. Clearly the release of latent heat did not cause a dramatic increase in vertical air motion in general.

6. CLOUD STRUCTURE

a) Cumulus Clouds

In order to reveal the pattern of airflow within and around individual clouds, gust vectors were constructed using 5 second means of alongwind (u) and vertical (w) velocities. (The mean wind direction was taken to be fixed over each of the periods sampled). The means of these velocity components over the period around the time the cloud was sampled (about 10 minutes in length) were then subtracted and the resulting fluctuation sets used to construct the vectors. The airflow within and around the cloud (on scales 25-50 m) was then compared to observed features of the droplet field and the distribution of smaller scale turbulence. Figures 9, 10 and 11 are examples of clouds analysed in this way.

The first cloud sampled on the 18 was a medium sized cumulus which was observed to be growing strongly (Fig. 9). Large variations in cloud base were evident (between about 1000 and 1350 m) with a narrow cleft in the centre of the

cloud seperating two strong updraught areas observed at both 1158 and 1386 m levels. The air motion within the cloud was predominately upwards (w_{max} about 4 ms^{-1} at both 1158 and 1386 m) with a downdraught region ahead of the cloud (w_{min} about -3 ms^{-1}) of approximately the same alongwind dimension as the cloud itself. The σ_w^2 trace shows that in both up and downdraughts there were short periods of order 20 seconds ≡ (100 m) when small scale turbulence was much higher than the mean. The distribution of liquid water within this cloud is similarly highly variable, with variations apparently occurring on a range of scales. Large fluctuations (much larger than the expected random sampling errors) in q_L occurred on a scale close to the resolution of the droplet measurements and regions with very low droplet concentrations only a few metres across were found well above the cloud base eg. at 122020 and 122153. Droplet data with a horizontal resolution of say 100 m (typical of data obtained using aircraft) would therefore tend to seriously underestimate the variability in q_L in similar clouds.

The cumulus clouds which formed during the early part of the observation period on the 19 were much smaller than those on the 18. Data obtained in the vicinity of three of these cumuli is shown in Fig. 19 and illustrate clouds of different sizes and in different stages of development. The cumulus sampled around 0942 GMT was dissipating rapidly and the gust vectors indicate that no updraught was within it at the level sampled and there was descent beneath it. The small wisp of cloud around 0944 GMT formed in the vicinity of the ASSP and uppermost turbulence probe. Although no updraught was observed at the top level there was a region of strong updraught at the level below. The wisp grew rapidly in the following few minutes to occupy a horizontal area several times larger than shown in Fig. 10 and it is interesting to speculate that this subsequent growth was due to the rising "bubble" beneath reaching it's condensation level. The larger cloud between 0946 and 0948 GMT represents a more classical picture of a cumulus than those described above as it had an approximately constant base height (to within the resolution of the observations, ± 50 m) and a "top hat" cross section of liquid water content. Telford (1975)

describes both these features as being typical characteristics of small cumulus.

On the 21, the cumuli were on average both smaller and shallower than on the other two days (see Figs 1 and 7). A cloud which was intercepted close to its base level is shown in Fig 11. This cloud, along with the one previously described in Fig 10 had a base level above the updraught centre slightly higher than that near the cloud edges (see also I). Peaks in the σ_w^2 occurred around the updraught area although the highest peak occurred in a region of low vertical velocity (see also I). Also the cloudy downdraughts were more turbulent than downdraughts, of similar vertical velocity in clear air. Three separate areas of cloud close to the level of the base were intercepted by the ASSP (marked A, B, C in Fig. 11) and there were clear differences in the droplet spectra characteristics between them. In the area sampled at around 1101 GMT, ie. closest to the cloud centre, the peak liquid water content and concentration were higher than in regions nearer to the cloud edges. Also, the dispersions of the droplet spectra were .35 ± .05 in the region A, .24 ± .04 near to the centre (B), and .28 ± .04 at the trailing edge (C). It is reasonable to suggest that parcels of cloudy air sampled near to the edges of the cloud (A and C) had travelled further since condensation initially occurred within them than regions of cloud sampled near to the main updraught (B). They would therefore be expected to have been exposed to the effects of mixing for a greater time and Baker et al (1981) have suggested that mixing between cloudy and clear air may be a cause of spectral broadening (ie. increased dispersion). Further evidence of differences in the amount of mixing comes from examination of the droplet concentrations in the different regions. Both peak and mean concentration were lower in regions A and C than in B. These observations demonstrate that droplet spectra measured at the same height can be different in shape, depending upon their location within the cumulus cloud. Caughey and Kitchen (1983) found spatial variations in nocturnal stratocumulus droplet spectra which were attributed to spectral modification by growth of

droplets near to cloud top due to radiative loss. In small cumulus, it is unlikely that radiative growth is a significant process in determination of the droplet spectrum as the time for which droplets are required to be within the layer of longwave flux divergence near to cloud top is of the order of minutes (Caughey et al 1982), ie. comparable to the cloud lifetime. The most probable reason for the variations is that adjacent parcels of cloudy air have different time histories, condensation having occurred in different areas of cloud base. The parcels are subsequently transported along different paths and subject to different amounts of mixing with cloud free air from outside the cloud. This conclusion emphasises that high resolution droplet data is essential in studies of spectral evolution. If the sample period is too long, measured droplet spectra may have spurious characteristics because each sample consists of regions of cloud with different spectral characteristics. This point can be demonstrated by illustrating the variability in spectral shape occurring over short timescales within this cloud. In Fig. 12 are plotted the mean spectra over the time period 110019 to 110029 GMT along with two out of the ten individual spectra which formed the mean. It can be seen that the slightly bi-modal mean spectrum is completely unrepresentative of those spectra measured at 110023 and 110026 GMT and that a considerable change in spectral shape occurred over times of a few seconds (equivalent to horizontal distances of a few tens of metres).

b) Stratocumulus Cloud

The stratocumulus cloud which formed later during the 19 was not uniform in appearance, with variations in cloud base height of the order of a few hundred metres (see Fig. 1). Examination of the vertical velocity time history within cloud revealed no organised convective motions like those found by Caughey and Kitchen (1983) in a nocturnal stratocumulus layer. The droplet spectra measured at a particular level were very variable and Table 6 presents a comparison of mean values of 1s parameters from short level runs near to cloud top and cloud base. The concentration was more variable near to cloud top, evidence of

the effects of mixing in of dry air from above the inversion. The two factors $\sigma_N/\overline{N}$ and σ_{RV}/R_V^3 are a measure of the variations in q_L due to variability in concentration and mean volume radius respectively. The relative magnitudes of these quantities suggests a highly inhomogenous structure near to cloud top with only small variations in mean radius but large changes in the droplet concentration. Near to cloud base, variations in mean volume radius account for about half the variability in q_L. This difference is probably not a result of the effects of mixing near to cloud base being different to those near to cloud top, but rather the variations in condensation level have a large effect on mean radius measured just above the cloud base. An extreme example of this effect can be seen in Fig. 13, where time histories of mean droplet radius and liquid water content are shown for a period when the stratocumulus base was variable with the ASSP eventually emerging from below cloud base. Although all samples were obtained at the same level the results are similar to those which would be obtained from profiles through a horizontally uniform cloud layer, with a steady increase in mean droplet radius with height. In the interpretation of droplet data where no estimates of local base height are available, care must be taken to avoid attributing spectral variations arising from such variability in cloud base height to other causes.

c) Mixing between cloudy and clear air

In recent studies of shallow convection, the results of mixing between cloudy and clear air has been described as inhomogeneous in that the horizontal variability of droplet spectra has followed the predictions of Latham and Reed (1977) (see eg. I, Caughey et al 1983, Slingo et al 1982a and b). The inhomogeneous model of mixing has been further developed (Baker et al 1981, Baker and Latham 1982) to show the effects of changes in some environment parameters on the degree of variability of the droplet spectra. The three key parameters which determine this droplet spectra variability according to Baker et al (1981) are:-

(i) The humidity of the air entrained into cloud, upon which the characteristic time for droplet evaporation T_R depends.

(ii) The level of turbulence within cloud, which determines the time scale for entrained volumes of air to be diffused throughout the cloud.

(iii) The size of the entrained volumes which, along with (ii) determines the time scale for erosion of entrained undersaturated parcels, τ_T.

In Blyth et al (1980) and Baker and Latham (1982), this model has been tested by comparing the predictions with observations in different case studies and it appears capable of simulating most of the variability in droplet spectra due to mixing. No indication was given however, that there were significant differences between the variability measured in different observational studies. The sensitivity of the model to different conditions therefore remains in some doubt. Using the present data, it is possible to determine whether significant differences in the spectral variability were evident in the different conditions.

The essential prediction of the inhomogeneous mixing theory is that as τ_T/τ_R increases, then fluctuations in the droplet concentrations rather than changes in spectral shape, will account for an increasing fraction of the variance in liquid water content. The relative contributions to the variance are given by $\sigma_N/\overline{N}$ and σ_{RV}/R_V^3. For each of the cloud traverses in the case studies, these two quantities have been calculated and plotted against each other in Fig. 14. No attempt has been made to exclude regions where cloud base is varying from the statistics (see above) because cloud base height (see Fig. 13) variations occurred in a large fraction of the traverses and also changes of up to 50 m would remain undetected. Unfortunately the result is that the values of σ_{RV} are probably overestimates of the variations in mean radius due to mixing. Nevertheless, for almost every traverse $\sigma_N/\overline{N} > \sigma_{RV}/R_V^3$ demonstrating that, as in previous studies, fluctuations in q_L were mainly due to fluctuations in N. There was considerable scatter in the ratio of $\sigma_N/\overline{N}$ to σ_{RV}/R_V^3 in all of the studies and this analysis revealed no evidence of systematic differences in the effects of mixing upon the cloud droplet population.

There is some evidence however of differences in the ratio τ_T/τ_R between the cases. From the formulation of τ_T and τ_R given in Baker et al (1981),

$T_T \propto \varepsilon^{-\frac{1}{3}}$ for a given scale of entrained volumes of cloud free air

and $T_R \propto q/q_s$ for a given mean droplet radius.

Assuming that the entrainment of air into cloud occurred across the cloud top then q may be taken as the humidity mixing ratio of air above the inversion layer. The available data suggests that, for a given entrainment scale and mean droplet radius, the ratio T_T/T_R on the 21 was approximately twice that on the 19, largely as a result of the dryer air above the inversion on the 21. As the cloud and CBL structure represented by these studies is typical of shallow convection over land, it is likely that the values of the ratio T_T/T_R are also typical. (The absolute values of T_T/T_R cannot be estimated because of the unknown entrainment scale). We therefore conclude that in order for observable differences in the nature of variations in spectral shape to occur, studies with a range of T_T/T_R greater than those encountered here must be considered.

7. CONCLUSIONS

These three case studies of shallow cloud in the CBL have provided information, of a mainly qualitative nature, of the relationship between cloud and CBL structure. The importance of subsidence and advection in boundary layer and cloud development suggest that combined aircraft and balloon data would be desirable in providing a more complete CBL heat and moisture budget. A possible feedback mechanism between cloud cover and entrainment rate, via the surface heat flux was identified in one of the studies, but much more complete measurements are required to study such relationships in detail.

The high resolution droplet data proved invaluable in identifying variations in droplet spectra occurring over horizontal scales of a few tens of metres. This highlights the importance of resolving the length scales associated with processes which modify the spectral shape, and care is needed in interpretation of data obtained from samples which have a length greater than these scales. One source of variation was the height of the observations above the local cloud base.

No significant differences were detected between the different cases in the effect of mixing of cloudy and clear air upon the variability in droplet spectra. In order to verify some of the predictions of the inhomogeneous mixing model therefore, a much greater range of cloud environments must be considered than those found in the present studies.

9. ACKNOWLEDGEMENTS

The authors wish to thank those members of staff of the Cloud Physics and Boundary Layer research branches of the Meteorological Office who took part in the project. In particular Messrs. A N Bentley, G Cooper, C Taylor and J Turton assisted in the field observations. The satellite photographs were supplied by the University of Dundee dept of electronics. During the data analysis, guidance and advice were provided by Drs. P Ryder and P Jonas.

LIST OF SYMBOLS

E_o	Latent heat flux at the surface (Evaporative heat flux)
E_i	" " " " " inversion base
N	Cloud droplet concentration
q	Humidity mixing ratio
q_{ad}	Adiabatic liquid water content
q_L	Liquid water content
q_s	Saturation humidity mixing ratio
R	Mean droplet radius
R_V	Mena volume radius
S_o	Incoming solar radiation measured at the surface
s	Distance upwind
t	Time
T	Temperature
$\overline{U}$	Mean Horizontal windspeed
u	Velocity in the direction of the mean horizontal wind velocity
v	" perpendicular to the direction of u
w	Vertical velocity
w_e	Entrainment velocity (defined as positive upwards)
w_s	Subsidence velocity (" " " ")
z	Height above ground
z_b	Cloud base height
z_i	Inversion base height
α	Ratio q_L/q_{ad}
Δq	Humidity mixing ratio step across the inversion (Taken as $q(z_i)$) - q_{min} in the layer 50 mb above z_i
ΔT	Temperature step across the inversion
ε	Dissipation rate of turbulence kinetic energy
θ	Potential Temperature
θ_e	Equivalent potential temperature

σ_R Dispersion of the droplet radius spectrum (expressed as a fraction of the mean radius)

σ_{RV} Standard deviation of R_V^3

σ_w^2 Vertical velocity variance

τ_R Characteristic time for droplet evaporation

τ_T " " " turbulent erosion of entrained volumes of air.

REFERENCES

Baker, M B and Latham J. 1982 A diffusive model of the turbulent mixing of dry and cloudy air, Quart. J. R. Met. Soc., 108, 871-898.

Baker, M B, Corbin, R G and Latham, J 1980 The influence of entrainment on the evolution of cloud droplet spectra. I. A model of inhomogeneous mixing, Quart. J. R. Met. Soc., 106, 581-598.

Blyth, A M, Choularton, T W, Fullarton, G, Latham, J, Mill, C S, Smith, M H, and Stromberg, I M 1980 The influence of entrainment on the evolution of cloud droplet spectra. II. Field experiments at Great Dun Fell. Ibid., 106, 821-840.

Brost, R A, Lenschow, D H and Wyngaard, J C 1982 Marine stratocumulus layers: Part 1: Mean conditions. J. Atmos. Sci., 39, 800-817.

Caughey, S J, and Palmer, S G 1979 Some aspects of turbulence structure through the depth of the convective boundary layer. Quart. J. R. Met. Soc., 105, 811-827.

Caughey, S J, Crease, B A and Roach, W T 1982 A field study of nocturnal stratocumulus: II Turbulence structure and entrainment. Ibid., 108, 125-144.

Caughey, S J, and Kitchen, M 1983 Simultaneous measurements of the turbulent and microphysical structure of nocturnal stratocumulus cloud, To be submitted to Quart. J. R. Met. Soc.

Coulman, C E, and Warner, J 1977 Temperature and humidity structure of the sub-cloud layer over land Boundary-Layer Met., 11, 467-484.

Emmitt, G D 1978 Tropical cumulus interaction with and modification of the sub-cloud region J. Atmos. Sci., 35, 1485-1502.

Kitchen, M and Caughey, S J 1981 Tethered-balloon observations of the structure of small cumulus clouds, Quart. J. R. Met. Soc., 107, 853-874.

Latham, J and Reed, R L 1977 Laboratory studies of the effects of mixing on the evolution of cloud droplet spectra. Quart. J. R. Met. Soc., 103, 297-306.

Lemone, M A and Pennel, W T 1976 The relationship of trade wind cumulus distribution to sub-cloud layer fluxes and structure. Mon. Wea. Rev., 104, 524-539.

Ludlam, F H 1980 Clouds and storms, Pennsylvania State Univ. Press. 405pps.

MacPherson, J I and Isaac, G A 1977 Turbulent characteristics of some Canadian cumulus clouds. J. Appl. Met., 16, 81-90.

Purser, R J, and McQuigg, R 1982 A successive correction analysis scheme using recursive numerical filters. Meteorological Office Met O 11 Technical Note No 154.

Roach, W T 1983 On the correlation between cloud top height and integrated liquid water path. In preparation.

Roach, W T, Brown, R, Caughey, S J, Crease, B A and Slingo, A 1982 A field study of nocturnal stratocumulus: I Mean structure and budgets. Ibid., 108, 103-124.

Silayeva, V I and Shmeter, S M 1977 Turbulence within cumulus clouds and outside them. Trent. Aerol. Obs., T. Vyp. 128, 63-72.

Slingo, A, Brown, R and Wrench, C L 1982a A field study of nocturnal stratocumulus: III High resolution radiative and microphysical observations. Quart. J. R. Met. Soc., 108, 145-166.

Slingo, A, Nicholls, S and Schmetz, J 1982b Aircraft observations of marine stratocumulus during JASIN, Quart. J. R. Met. Soc., 108, 833-856.

Telford, J W 1975 Turbulence, entrainment and mixing in cloud dynamics. Pure Appl. Geoph., 113, 1067-1984.

Telford, J W and Wagner, P B 1980 The dynamical and liquid water structure of the small cumulus as determined from its environment. Pure Appl. Geoph, 118, 935-952.

Warner, J 1969 The microstructure of cumulus clouds, part I: General features of the droplet spectrum. J. Atmos. Sci., 26, 1048-1059.

Warner, J 1969a Part II: The effect on droplet size distribution of the cloud nucleus spectrum and updraft velocity. Ibid., 26, 1272-1282.

Warner, J 1970 Part III: The nature of the updraught. Ibid., 27, 682-688.

Warner, J 1973 Part IV: The effect on the droplet spectrum of mixing between cloud and environment. Ibid., 30, 256-261.

Warner, J 1981 On mixing processes in cumulus clouds. Pure Appl. Geoph. 119, 809-815.

TABLE CAPTIONS

Table 1:- A comparison between the turbulence probes on the 19 over the time period 1343-1519 GMT. All three probes were adjacent at a height of 2 m above the surface.

Table 2:- Inversion data obtained from the uppermost turbulence probe. On the 18, no transits through the inversion were made.

Table 3:- Estimates of contributions to boundary layer growth from subsidence, advection and entrainment.

Table 4:- Surface insolation, evaporative heat flux and entrained moisture flux for 3 hour periods during the case studies. The errors are difficult to estimate and in the case of E_i, are probably large due to uncertainties in w_e.

Table 5:- A comparison of mean small scale (less than about 50 m) turbulence within, beneath and between clouds. All the values represent averages over at least 25 values of σ_w^2 computed over 6 second periods.

Table 6:- Mean droplet spectral characteristics from level runs near to cloud top and cloud base in stratocumulus patches on the 19.

TABLE 1

PROBE NO.	$\overline{U}$ (ms^{-1})	$\overline{T}$ (K)	σ_w^2 (m^2s^{-2})
1	3.55	280.22	1.72
2	3.63	280.11	1.54
3	3.87	280.07	1.27

TABLE 2

DATE	TRANSIT NO.	TIME (GMT)	z_i (m)	ΔT (^oC)
19/8/80	1	1038	1320	4.3
"	2	1100	1370	4.0
"	3	1129	1250	3.9
"	4	1219	1335	2.0
"	5	1222	1375	2.1
"	6	1237	1380	1.6
21/8/80	1	1111	1112	3.6
"	2	1216	1234	4.0
"	3	1352	1249	4.3
"	4	1410	1447	3.5

TABLE 3

DATE	TIME PERIOD (GMT)	dz_i/dt (ms^{-1})	w_s (ms^{-1})	$\overline{U}dz_i/ds$ (ms^{-1})	w_e (ms^{-1})
19/8/80	0900-1030	.06 ± .02	-.005 ± .005	0 ± .01	.07 ± .04
"	1030-1300	.006	-.005 ± .005	0 ± .01	.01 ± .02
21/8/80	1100-1500	.023	-.01 ± .01	.015 ± .005	.02 ± .02

TABLE 4

DATE	TIME PERIOD (GMT)	S_o (Wm^{-2})	E_o (Wm^{-2})	E_i (Wm^{-2})
18/8/80	1200-1500	330	170	-
19/8/80	0900-1200	420	230	245
"	1200-1500	310	170	35
21/8/80	1200-1500	690	230	225

TABLE 5

DATE	PROBE LEVEL	$\overline{\sigma_w}^2$ (m^2s^{-2}) BETWEEN CLOUDS	$\overline{\sigma_w}^2$ (m^2s^{-2}) WITHIN AND BENEATH CLOUDS
19/8/80	TOP	.02 ± .01	.07 ± .07
"	MIDDLE	.02 ± .02	.07 ± .10
"	BOTTOM	.02 ± .02	.12 ± .27
21/8/80	TOP	.02 ± .03	.18 ± .19
"	MIDDLE	.21 ± .23	.17 ± .15
"	BOTTOM	.38 ± .75	.29 ± .36

TABLE 6

TIME PERIOD (GMT)	HEIGHT ABOVE CLOUD BASE (m)	$\overline{q_L}$ (gm^{-3})	$\overline{N}$ (cm^{-3})	$\overline{R_V}$ (μm)	$\overline{\sigma_R}$	$\sigma_N/\overline{N}$	$\sigma_{RV}/\overline{R_V^3}$
112807-113135	200-400	.32 ± .21	298 ± 200	6.2 ± 0.6	.25 ± .05	.67	.29
124237-125400	0-200	.12 ± .10	424 ± 228	3.6 ± 1.0	.26 ± .06	.40	.37

FIGURE CAPTIONS

Fig 1:- Time height cross section of the balloon-borne instruments on the three days. The continuous lines mark the tracks of the turbulence probes. The outlines of the clouds which passed either through or directly above the instrument array are shown but it should be remembered that cloud base height was estimated to about $\pm$ 50 m and cloud top represents a visual estimate in most cases. The principal level runs on each day are marked A-E.

Fig 2:- A satellite picture of England and Wales taken at 1430 GMT on the 18. Cardington (marked by a cross) was in an area of cloud patches about 10 km across. The wind direction over the whole of the area was north westerly.

Fig 3:- Surface pressure analysis for 1200 GMT on the 19. Also shown is an analysis of low cloud amounts and the location of up and downstream radiosonde ascents.

Fig 4:- A satellite picture for the same area as Fig 2 taken at 1358 GMT on the 21. The variations in cloud amounts should be compared to the pattern of surface divergence Fig 6b. As on the 18 and 19, the wind direction over southern England was north westerly.

Fig 5:- Temperature, humidity and wind profiles from the 1100 GMT Crawley radiosonde ascents on the 18, 19 and 21. In this figure and others following a symbol convention has been adopted as follows:-

Δ 18 August

o 19 August before 1030 GMT (cumulus clouds at Cardington)

● " " after 1030 GMT (stratocumulus clouds at Cardington)

□ 21 August

The profiles of θ and $\bar{U}$ in the CBL measured at Cardington were similar to those measured at Crawley.

Fig 6:- a) An analysis of surface divergence at 1200 GMT on the 19. The weak pattern implies little subsidence over southern England. The units of divergence are $\times 10^{-5}$ s^{-1}.

b) The same as Fig 6a for 1200 GMT on the 21, There is some correspondence between the cloud free area shown in Fig 4 and an area of subsidence over southern England.

Fig 7:- The distribution of updraught and cloud scales. The histograms show the fractions of the total level run length in each of the case studies which was occupied by transits of updraughts and clouds of three scales

($\lesssim$ 1 km, >1 km but < 2 km, $\gtrsim$ 2 km).

Fig 8:- a) The vertical velocity variance calculated over the length of the level runs marked in Fig 1 as a function of the normalised height z/z_i.

b) The dissipation rate of turbulence kinetic energy as a function of normalised height. Data from the 18 were not available because of contamination of the high frequency vertical velocity fluctuations by probe oscillations (see section 2).

Fig 9:- Detailed measurements of a medium sized cumulus cloud on the 18. At the top of this figure are traces of cloud droplet parameters (dispersion, mean volume radius, concentration and liquid water content) at one second intervals. Below is the time height cross-section with 5 second gust vectors (in a vertical plane) from the three probe levels. The boundaries of the visible cloud are marked (~~~). In between, value of σ_w^2 computed over 6 second averaging periods at the 1386 m level shows horizontal distribution of small scale turbulence in the cloud layer.

Fig 10:- Same as Fig 9 but for three small cumulus clouds sampled on the 19.

Fig 11:- Same as Fig 9 but for a small cumulus cloud (and the downwind edge of the previous cloud) sampled on the 21.

Fig 12:- Three droplet spectra measured within the cloud illustrated in Fig 11. The error bars shown are the statistical errors in the measured concentration, rather than the absolute error.

Average spectrum 110019-110029 GMT

Spectrum measured at 110023 GMT

" " " 110026 GMT

Fig 13:- Mean radius and liquid water content measured close to the base of an area of stratocumulus on the 19. There was considerable variation in spectral shape over horizontal distances of a few hundred metres. The adiabatic liquid water content was estimated using visual estimates of cloud base height for comparison. The error bars shown represent uncertainty in the cloud base height. Possible errors arising from the correction of ASSP liquid water contents are not considered.

Fig 14:- The variability in droplet concentration ($\sigma_N/\overline{N}$) and the mean volume radius cubed ($\sigma_{RV}/\overline{R_v^3}$) for each cloud in the three case studies in all but two areas of stratocumulus on the 19, $\sigma_N/\overline{N} > \sigma_{RV}/\overline{R_v^3}$.

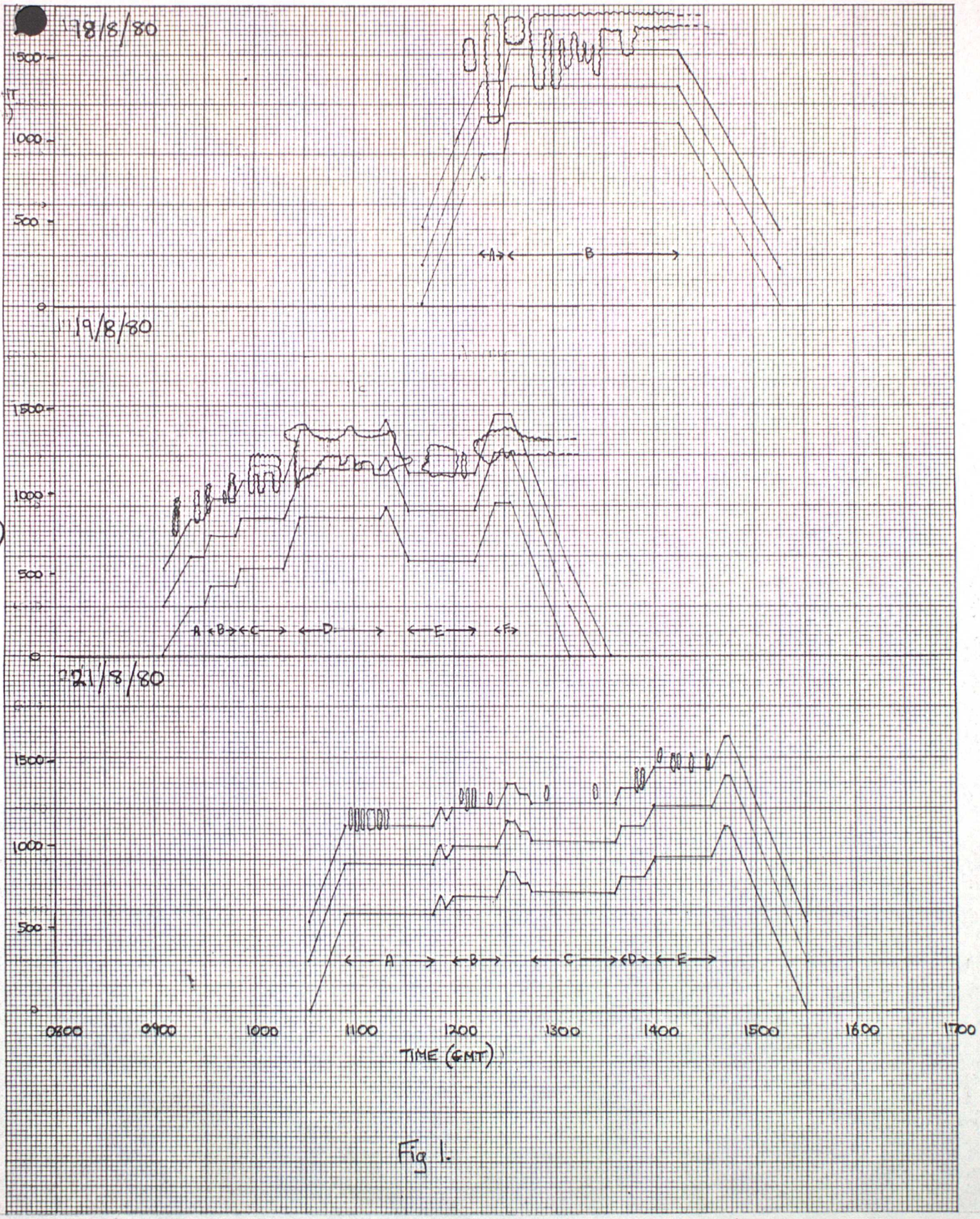
18/8/80
1500
1000
500
0
A
B
19/8/80
1500
1000
500
0
A
B
C
D
E
F
21/8/80
1500
1000
500
0
A
B
C
D
E
0800
0900
1000
1100
1200
1300
1400
1500
1600
1700
TIME (GMT)

Fig 1.

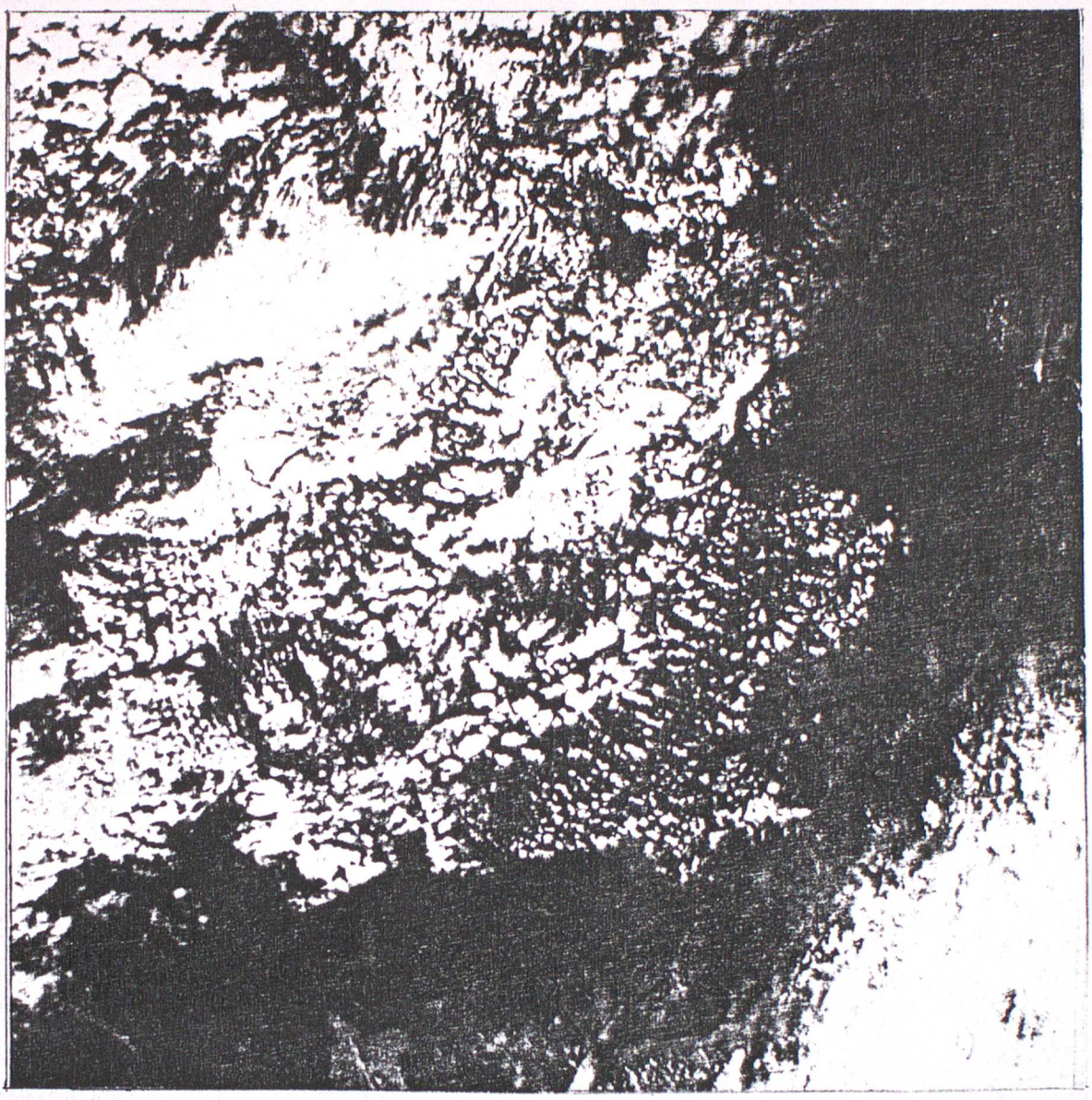

Fig. 2

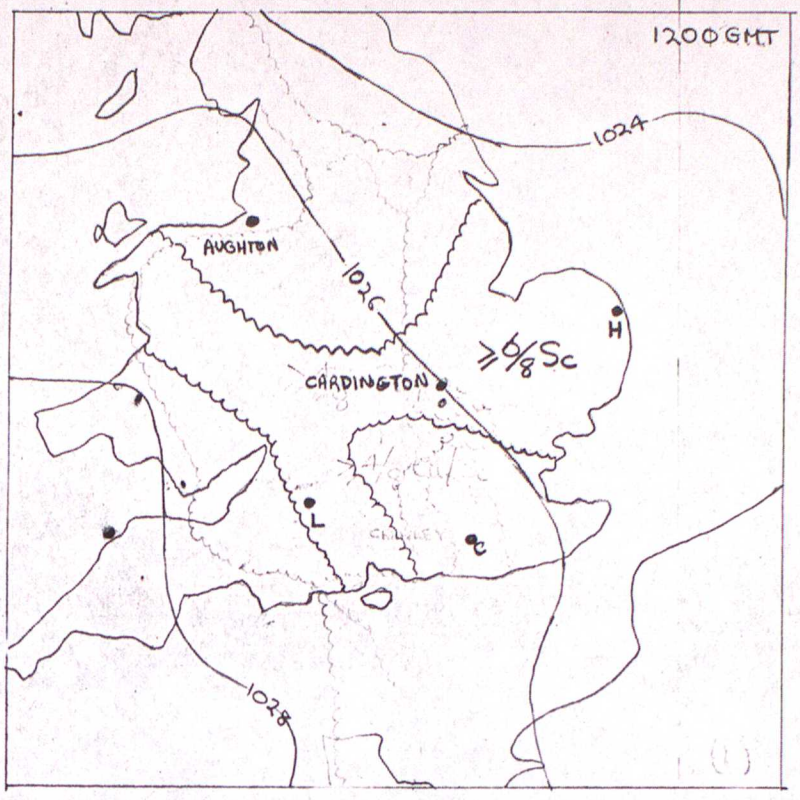

Fig 3

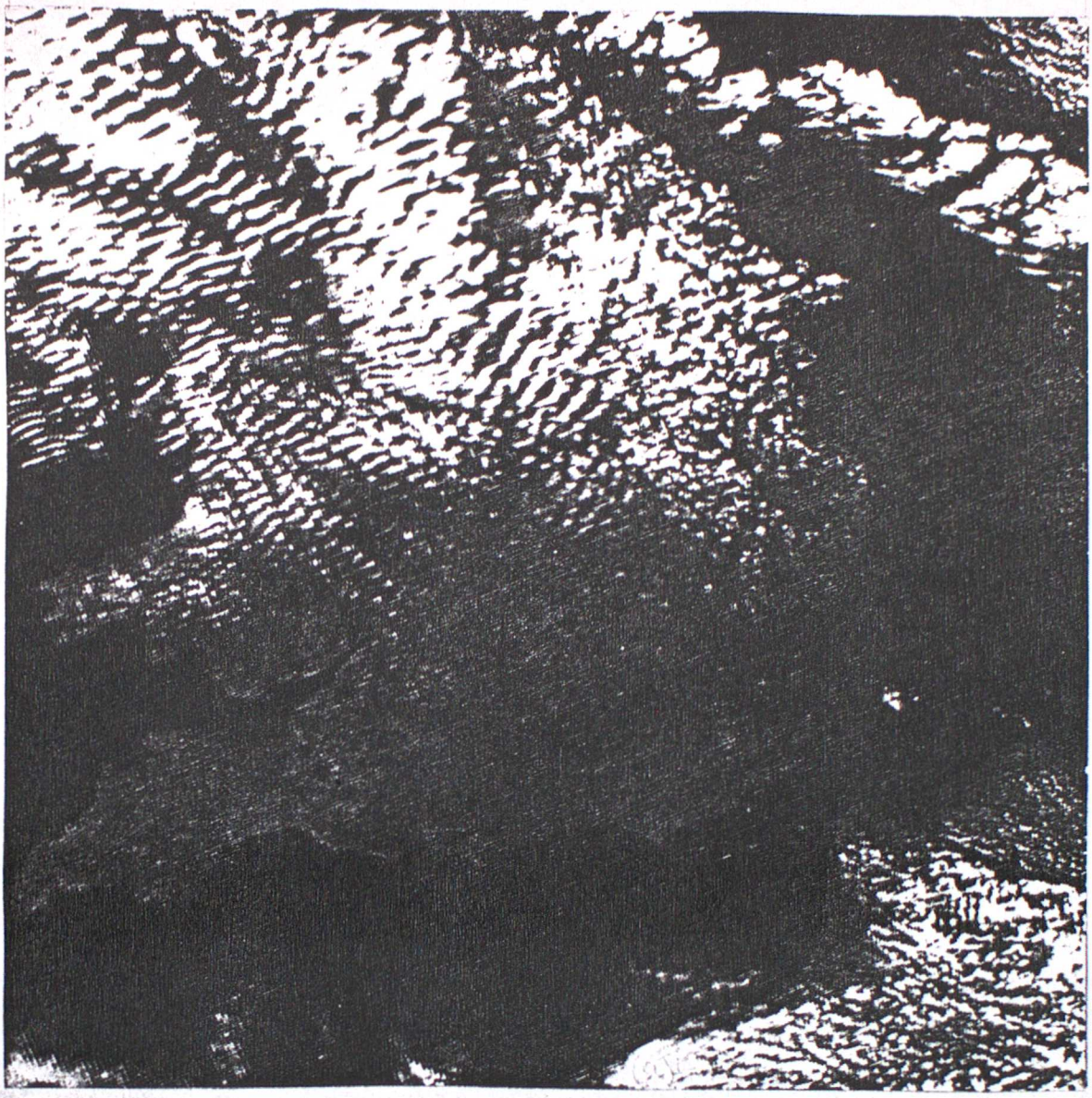

Fig 4

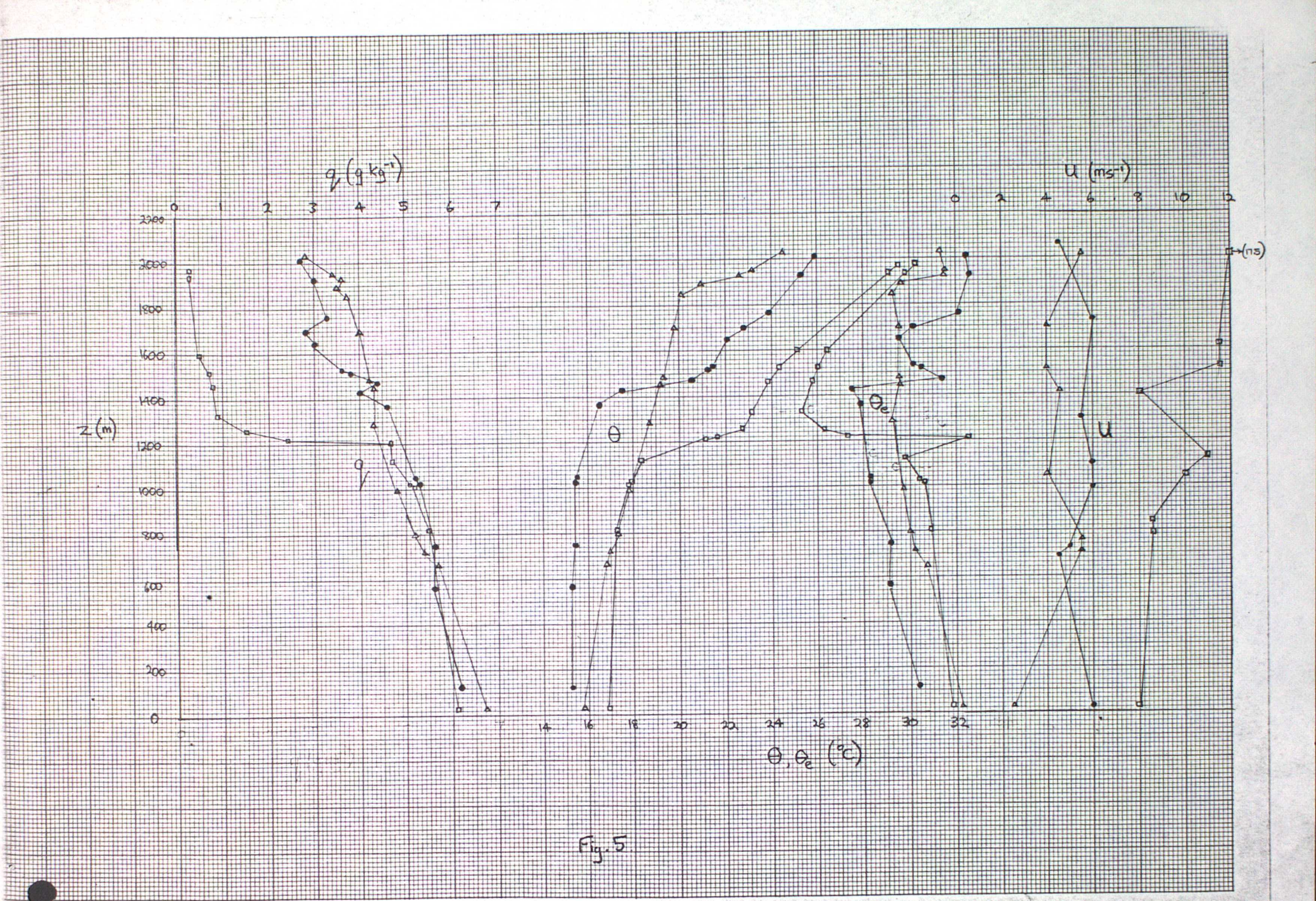
q (g kg⁻¹)
0 1 2 3 4 5 6 7
u (ms⁻¹)
0 2 4 6 8 10 12
(ms)
2200
2000
1800
1600
1400
1200
1000
800
600
400
200
0
z (m)
q
θ
θe
u
14 16 18 20 22 24 26 28 30 32
θ, θe (°C)

Fig. 5

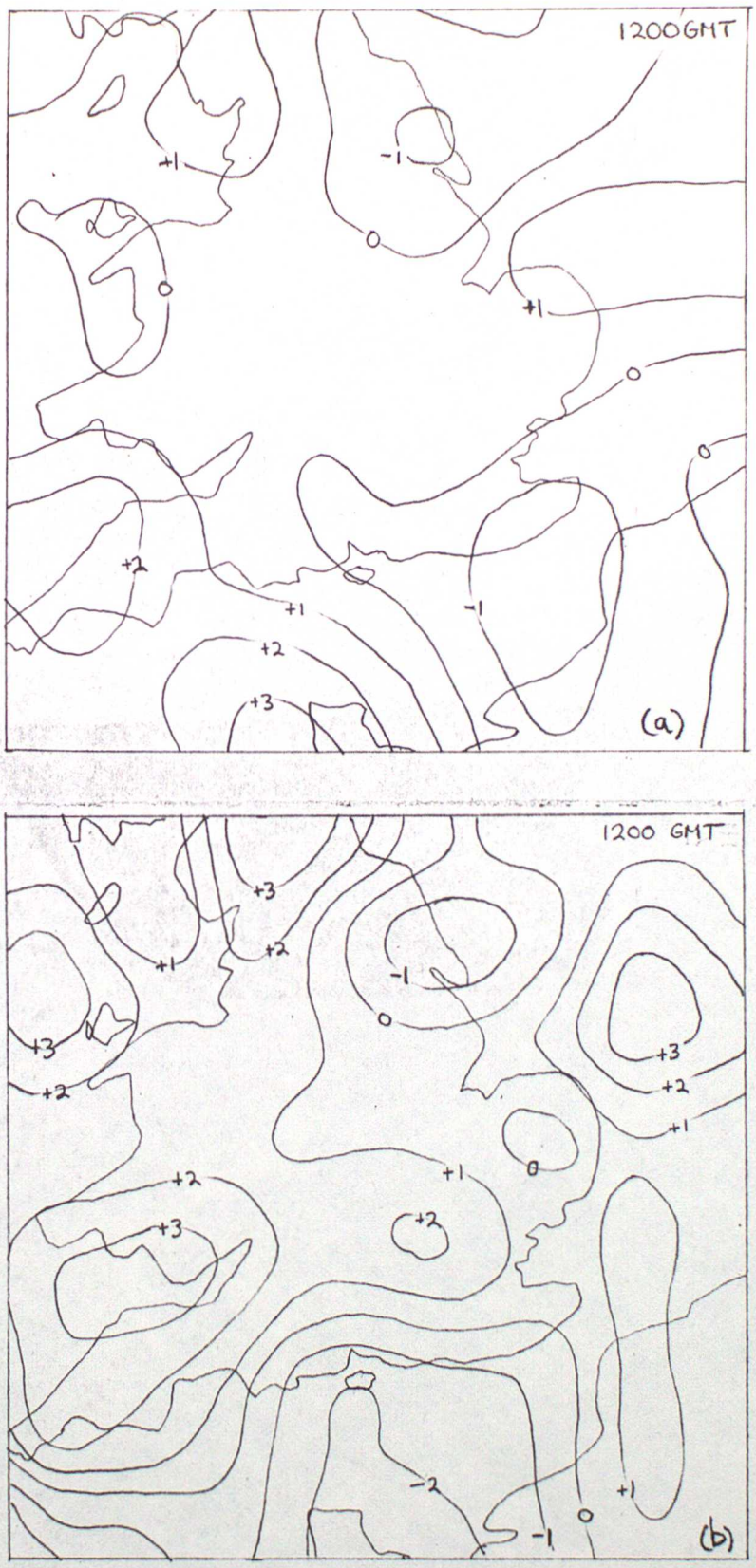

Fig. 6

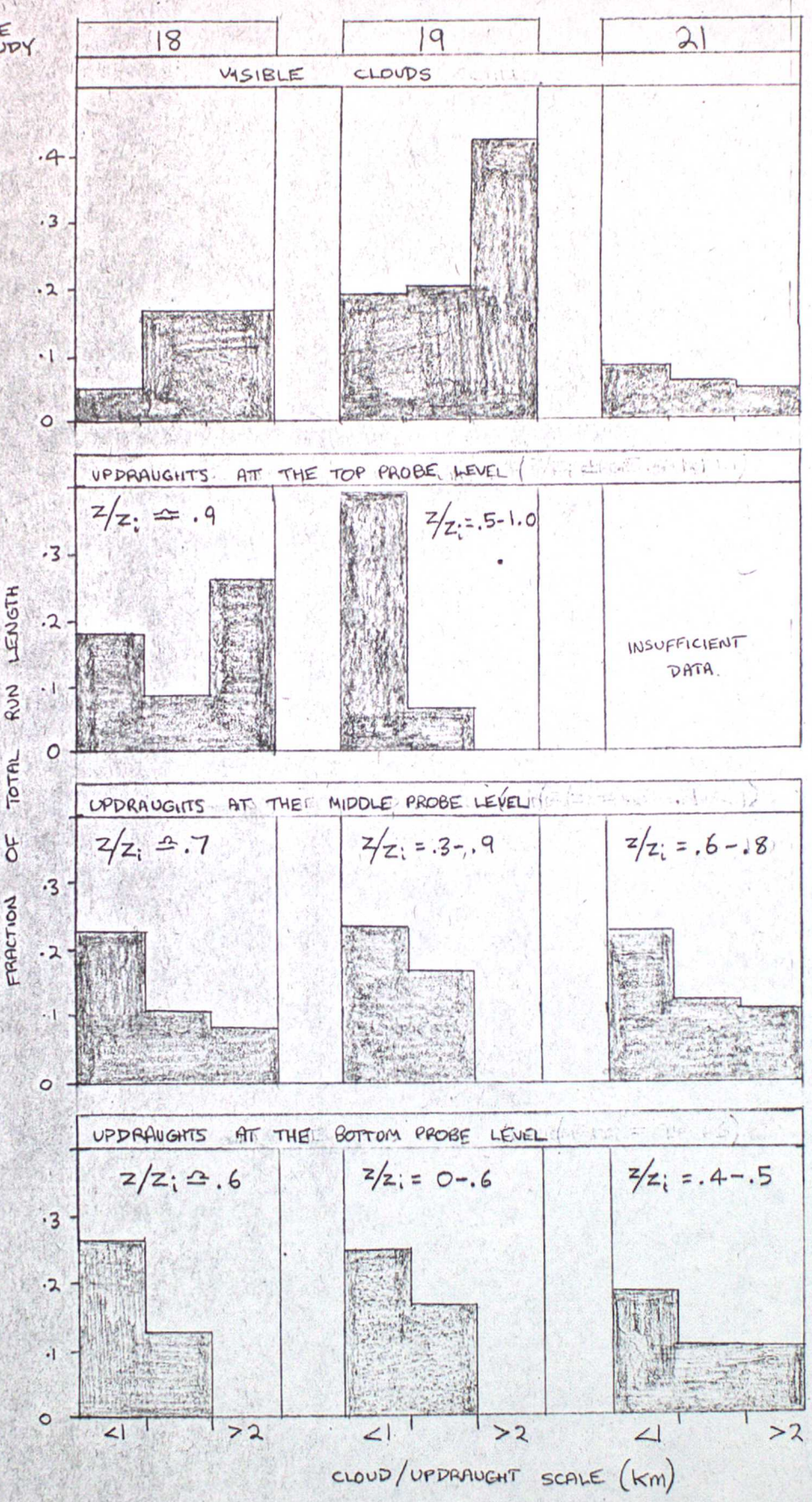
CASE STUDY
18
19
21
VISIBLE CLOUDS
UPDRAUGHTS AT THE TOP PROBE LEVEL
z/z_i ≏ .9
z/z_i = .5-1.0
INSUFFICIENT DATA.
UPDRAUGHTS AT THE MIDDLE PROBE LEVEL
z/z_i ≏ .7
z/z_i = .3-.9
z/z_i = .6-.8
UPDRAUGHTS AT THE BOTTOM PROBE LEVEL
z/z_i ≏ .6
z/z_i = 0-.6
z/z_i = .4-.5
FRACTION OF TOTAL RUN LENGTH
0
.1
.2
.3
.4
<1
>2
CLOUD/UPDRAUGHT SCALE (km)

Fig. 7

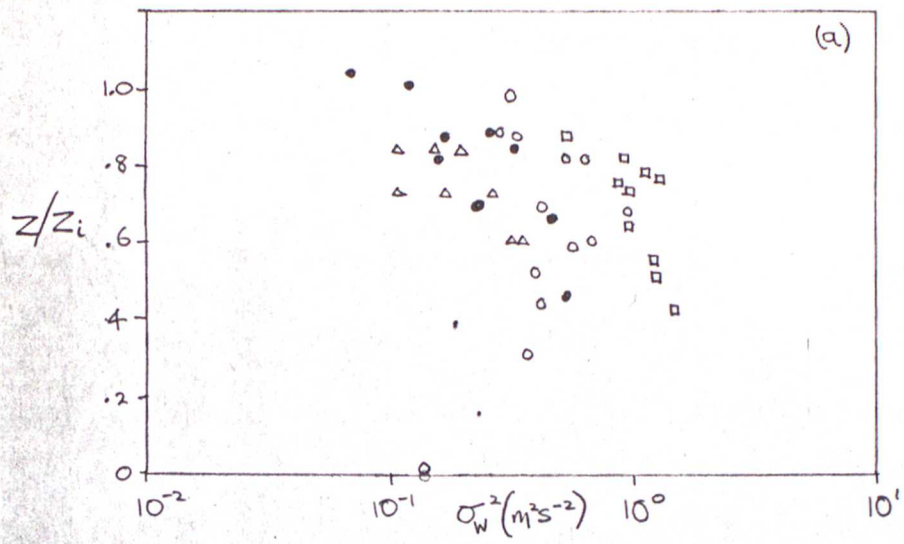
(a)
1.0
.8
.6
.4
.2
0
z/zi
10⁻²
10⁻¹
σw²(m²s⁻²)
10⁰
10¹

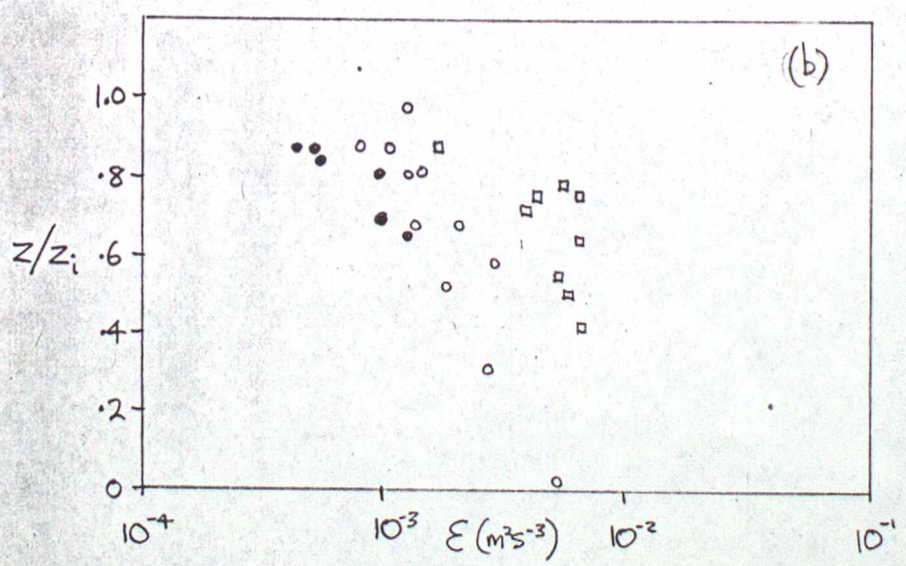
(b)
1.0
.8
.6
.4
.2
0
z/zi
10⁻⁴
10⁻³
ε(m²s⁻³)
10⁻²
10⁻¹

Fig 8

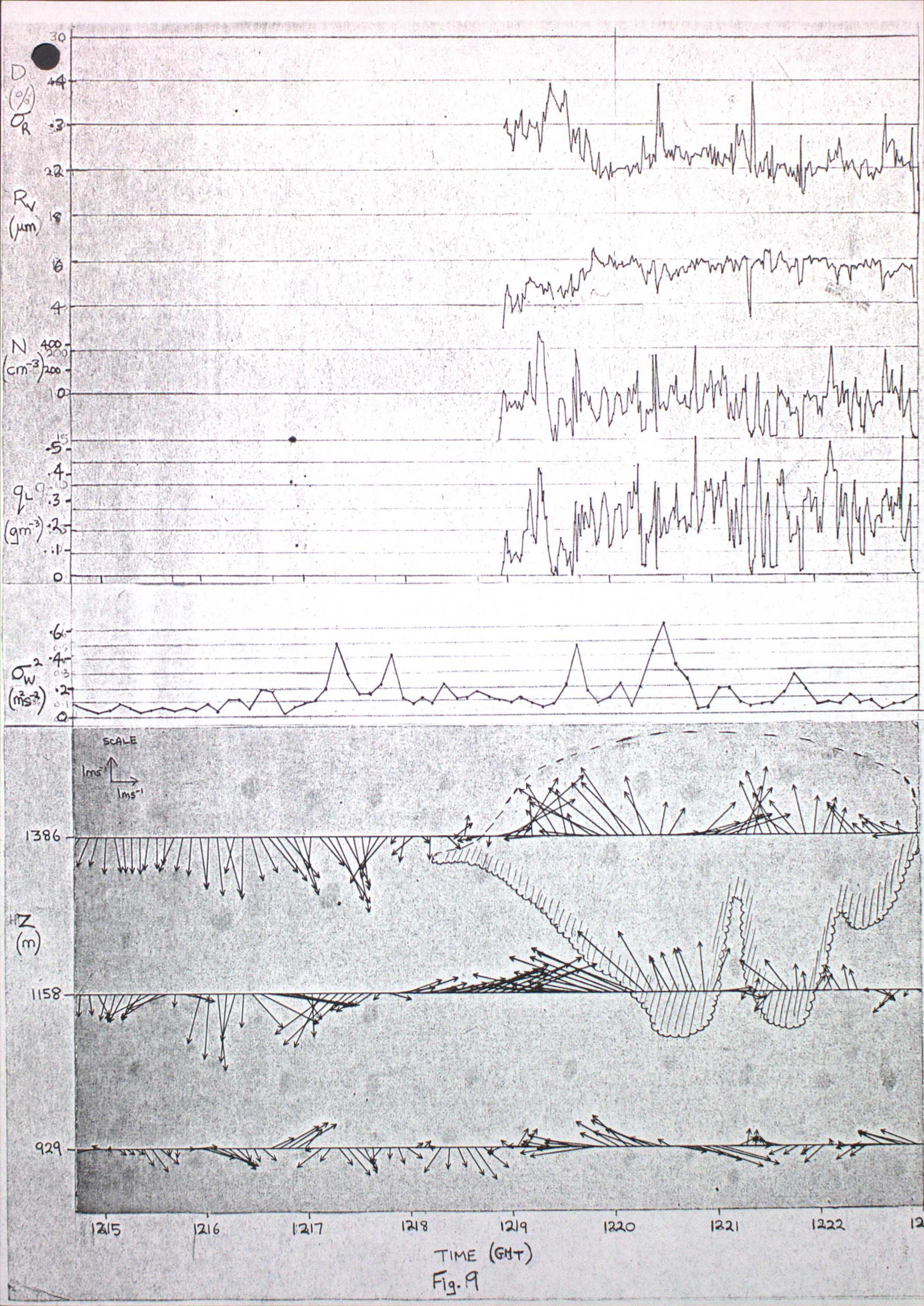
D (%)
σ_R
30
44
·3
22
R_V (μm)
18
16
4
N (cm^{-3})
400
200
200
100
q_L
·5
·4
·3
·2
·1
0
σ_W^2 ($m^2 s^{-3}$)
·6
·4
·2
0
SCALE
$1 ms^{-1}$
$1 ms^{-1}$
1386
HTZ (m)
1158
929
1215
1216
1217
1218
1219
1220
1221
1222
TIME (GMT)

Fig. 9

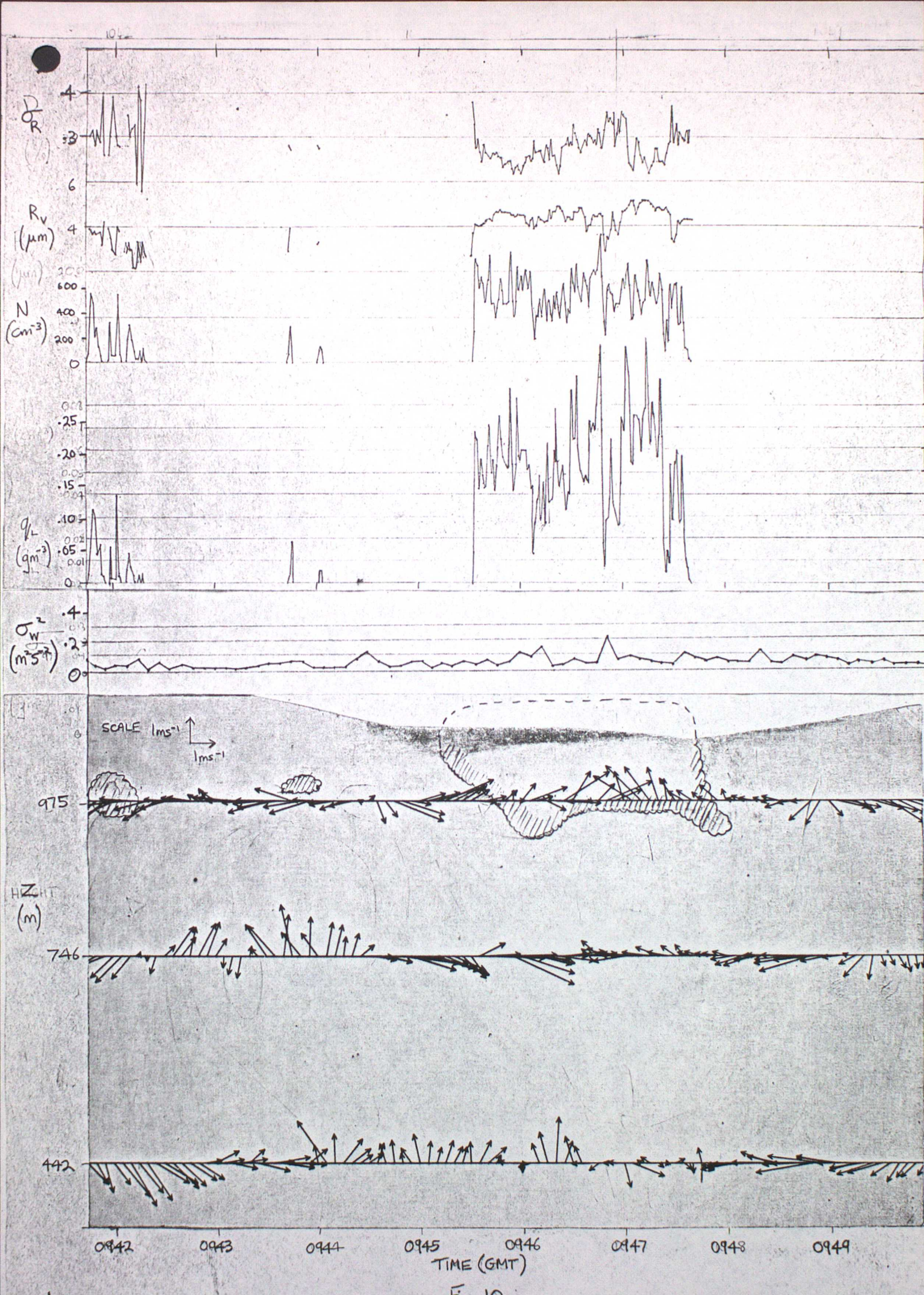
D_R (μm)
R_V (μm)
N (cm^{-3})
q_L (gm^{-3})
σ_w^2 ($m^2 s^{-2}$)
SCALE 1ms⁻¹
1ms⁻¹
975
746
442
HEIGHT (m)
0942
0943
0944
0945
0946
0947
0948
0949
TIME (GMT)

Fig. 10

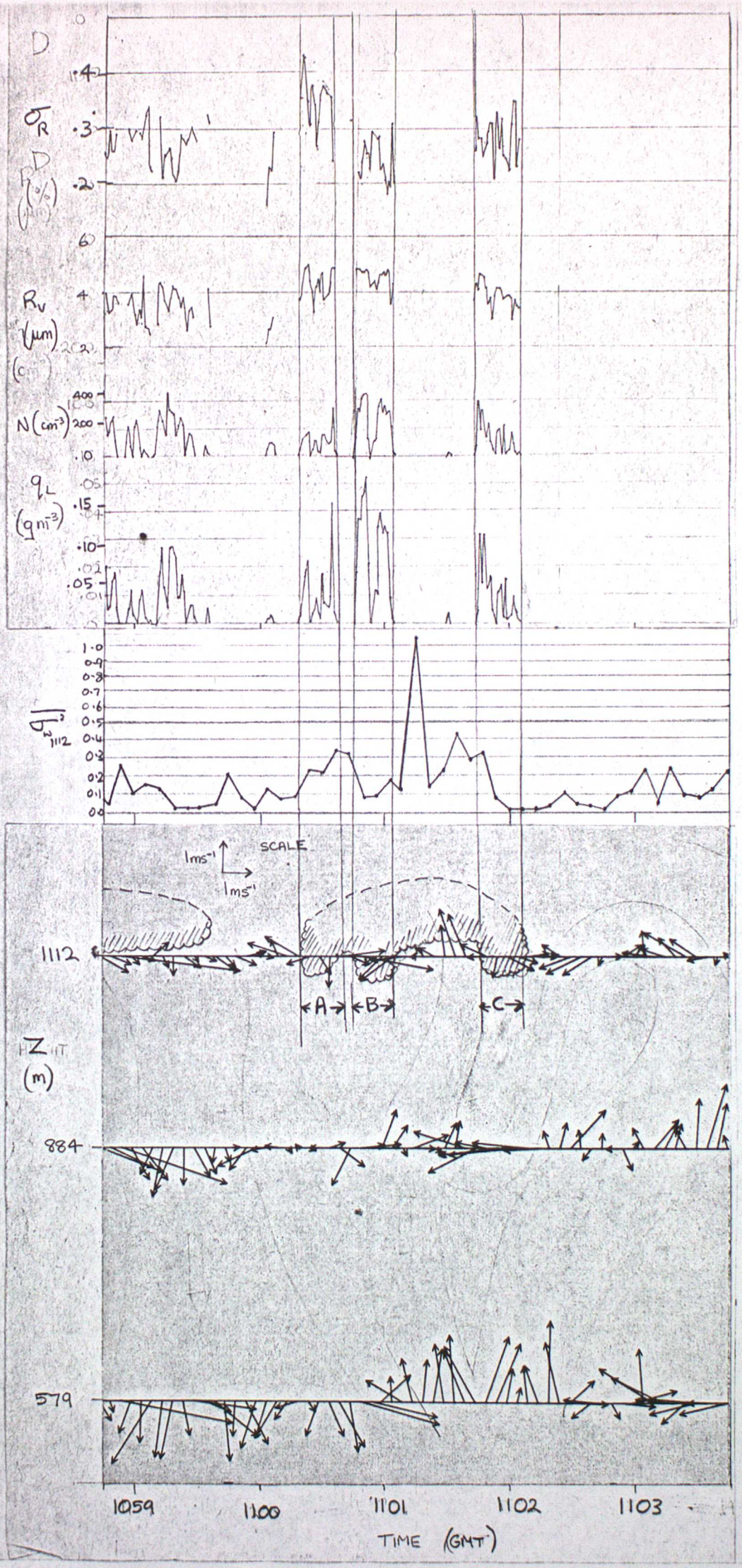
D
σ_R
D (%)
R_v (μm)
N (cm^{-3})
q_L ($g\,m^{-3}$)
$\overline{q_L}$ / $\overline{q_L}_{1112}$
SCALE
1 ms⁻¹
1 ms⁻¹
1112
A
B
C
HT (m)
884
579
1059
1100
1101
1102
1103
TIME (GMT)

Fig. 11.

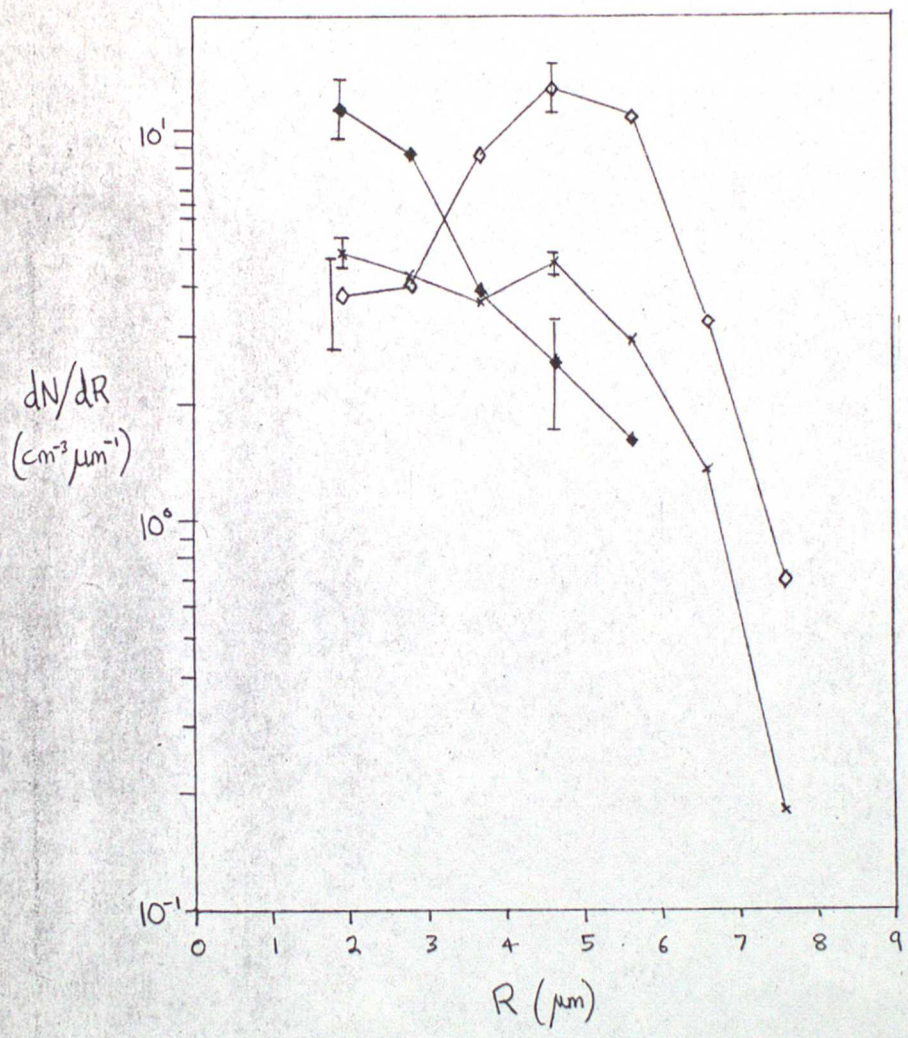

Fig. 12

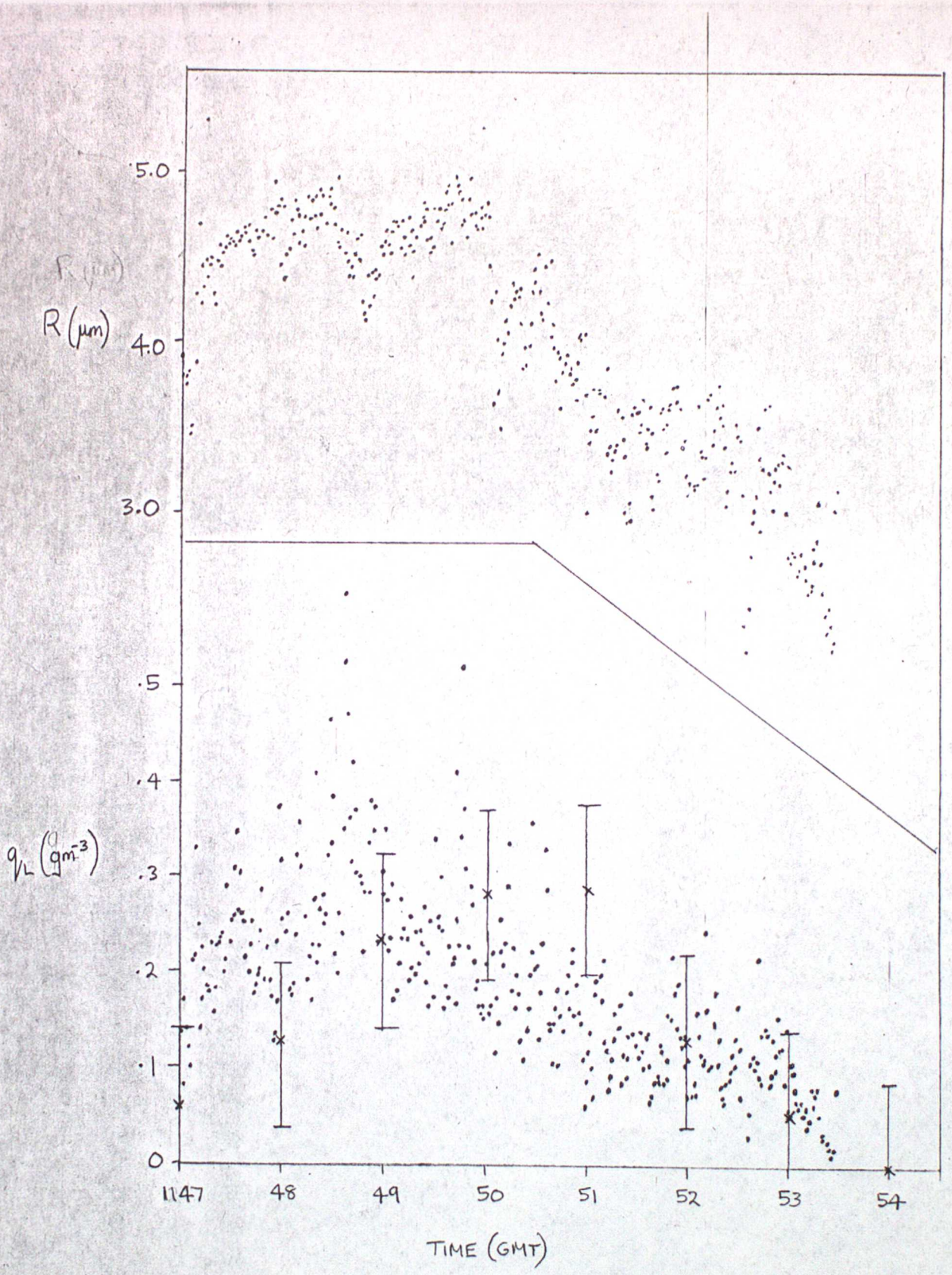

Fig. 13

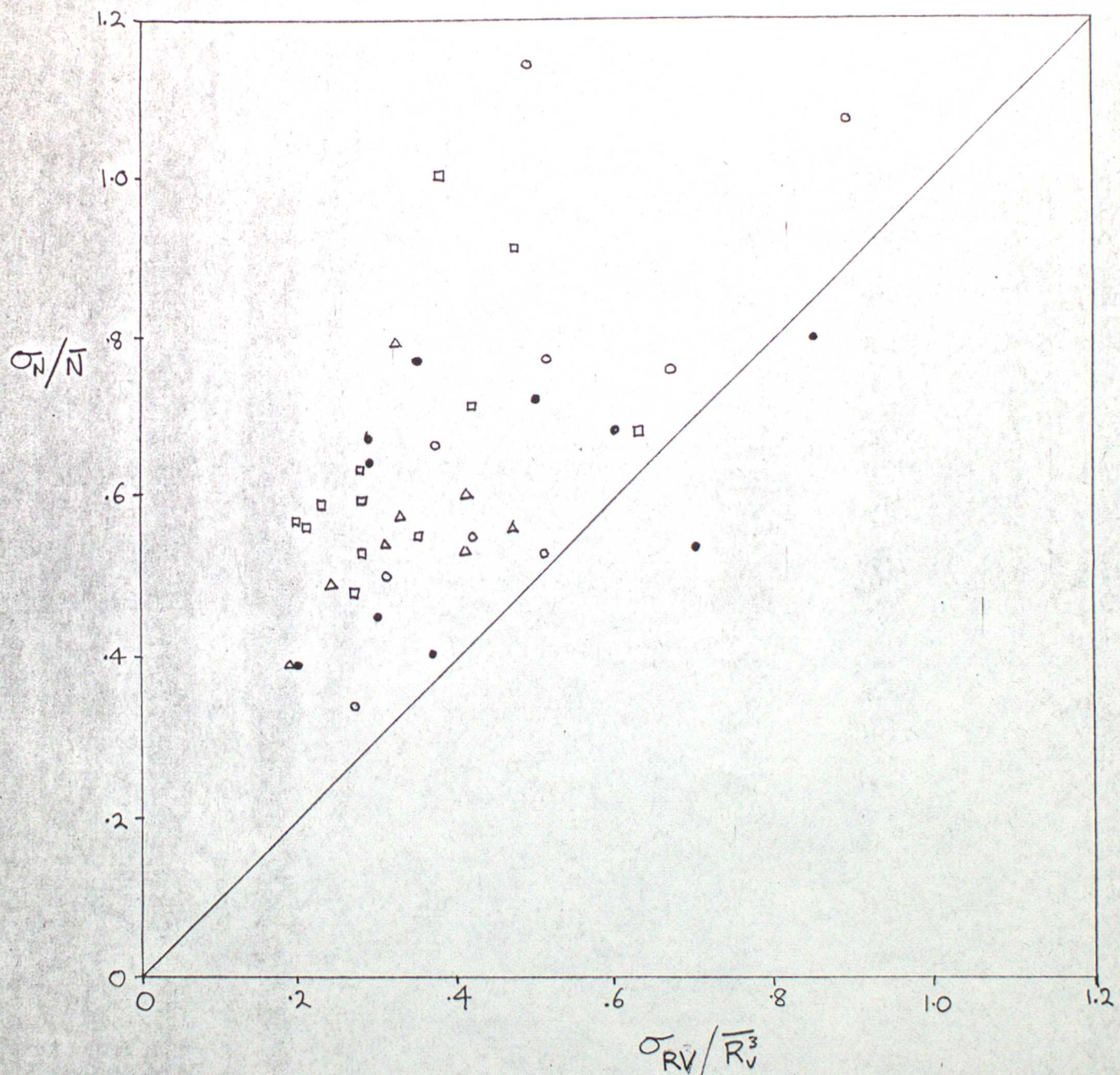

Fig. 14